Knockdown of BATF alleviates lung injury in septic neonates through transcriptional regulation of COTL1

JIHUI ZHANG, HUIMIN JIANG

Department of Emergency, People's Hospital of Ningxiang City, Ningxiang, Hunan, China

Abstract

Introduction: *Neonatal sepsis (NS) seriously threatens the health of infants. Coactosin-like protein 1 (COTL1) is a binding protein of F-actin and 5-lipoxygenase which is known to regulate the progression of neonatal sepsis. Nevertheless, the function of COTL1 in NS is not clear.*

Material and methods: *An in vivo model of NS was established using cecal slurry (CS). H&E staining was applied for observing the severity of lung injury in tissues of mice. MTT assay was applied for determining cell viability, and the inflammatory factors were examined using ELISA. Apoptosis was assessed via flow cytometry. Superoxide dismutase (SOD), malondialdehyde (MDA) and glutathione (GSH) levels were assessed by commercial kits. The interaction between basic leucine zipper ATF-like transcription factor (BATF) and COTL1 was verified using dual luciferase reporter and chromatin immunoprecipitation (ChIP) assay.*

Results: *COTL1 knockdown alleviated the progression of NS-induced lung injury. COTL1 knockdown enhanced the viability and decreased interleukin (IL)-6 and IL-1β levels in lipopolysaccharides (LPS)-stimulated pulmonary microvascular endothelial cells. Silencing of COTL1 inhibited LPS induced apoptosis and oxidative stress. More importantly, BATF activated MAPK/NF-κB signaling through transcriptionally upregulating COTL1. Furthermore, BATF improved the LPS-induced inflammatory response and apoptosis in pulmonary microvascular endothelial cells through mediation of COTL1.*

Conclusions: *BATF knockdown alleviated NS-induced lung injury by activating the MAPK/NF-κB pathway via transcriptionally upregulating COTL1 expression.*

Key words: *neonatal sepsis, oxidative stress, lung injury, COTL1, BATF.*

(Cent Eur J Immunol 2024; 49 (3): 238-251)

Introduction

Neonatal sepsis (NS) is systemic disease which is induced by viral, fungal or bacterial infections, and it ranks third among the leading cause of neonatal death [1, 2]. The symptom of NS includes systemic inflammation and multi-organ dysfunction [3]. In addition, the progression of sepsis tends to spread to the lung, and lung injury is the main feature of sepsis [4, 5]. Although various efforts have been made for the treatment of sepsis, the mortality of patients with sepsis remains high due to septic lung injury [6]. Hence, there is an urgent need to discover a novel method for alleviating the lung injury in NS.

Coactosin-like protein 1 (COTL1) is a cytoskeleton-associated protein with critical roles in cell migration, adhesion, and signaling, which is involved in the progression of tumors and inflammation [7]. For instance, Xia *et al.* reported that COTL1 suppressed breast carcinoma cell proliferation [8]; Tan *et al.* found that silencing of COTL1 could ameliorate myocardial ischemia/reperfusion injury [9]. The previous report indicated that sepsis is induced by inflammation [10], and upregulation of COTL1 could lead to inflammatory responses [11]. Meanwhile, the level of COTL1 was upregulated in serum of patients with sepsis [12]. Nevertheless, the detailed function of COTL1 in NS needs further analysis. On the other hand, MAPK/NF-κB (mitogen-activated protein kinase/nuclear factor κB) signaling was found to be a vital modulator in malignant tumors and inflammation [13, 14]. More importantly, MAPK/NF-κB acts as a modulator in sepsis [15]. The relation between MAPK/NF-κB and lung injury (or inflammation) has been previously illustrated. For instance, forsythiaside A could attenuate lung injury *via* suppressing inflammation through regulation of MAPK/NF-κB signaling [16]; fusidic acid derivatives attenuated injury in the lung by suppressing the MAPK/NF-κB pathway [17]. Meanwhile, it was re-

vealed that knockdown of COTL1 could inactivate the NF-κB and MAPK pathway to inhibit the progression of breast cancer [8]. Nevertheless, the association between COTL1 and MAPK/NF-κB in NS is unexplored.

After that, the upstream mechanism of COTL1 in NS was explored. Transcriptional factors often play vital roles in diseases through regulating the downstream mRNAs [18, 19]. In addition, basic leucine zipper ATF-like transcription factor (BATF) is a transcriptional factor which can regulate the progression of multiple diseases *via* modulating the downstream targets. For example, BATF could repress BIM to sustain tolerant T cells in the periphery [20]; BATF relieved hepatic steatosis by inhibiting PD1 and promoting energy metabolism [21]. Meanwhile, previous research found that BATF could aggravate sepsis-associated liver injury through transcriptional enhancement of GBP-5 [22]. BATF has been reported to inhibit lung injury [23], and it could also suppress the inflammatory response in hepatic steatosis [21]. The prediction of JASPAR indicated that COTL1 had binding sites with BATF, while the detailed relation between BATF and COTL1 in NS remains largely unknown.

Collectively, it is hypothesized BATF might aggravate NS-induced lung injury through transcriptionally enhancing COTL1 to activate MAPK/NF-κB signaling. This research might provide a new therapeutic target against septic lung injury.

Material and methods

In vivo experiments

C57BL/6 mice (5-7 days old, $n = 6$ per group) originated from Chinese Academy of Science (Shanghai, China). In addition, mice were assigned to Sham, cecal slurry (CS), CS + sh-NC and CS + sh-COTL1 groups. To mimic NS *in vivo*, mice were administered CS according to the previous report [24] (Supplementary Figure 1). For preparing CS, C57BL/6 mice (11-13 weeks old; 3 male and 3 female) were euthanized using CO_2 inhalation. Cecotomy and laparotomy were applied for collecting cecal contents. Dextrose (5%; Sigma, St. Louis, MA, USA) was applied for suspending the cecal contents in 90 mg/ml saline after weighing. Next, the CS was filtered to remove large particles, then the CS was frozen and stored at −80°C. To induce sepsis, neonates were kept at 37°C. Mice were anesthetized using isoflurane (2.5%, Beyotime, Shanghai, China) after CS was delivered through intraperitoneal injection. Sham mice were administered a similar procedure except for the injection of normal saline. After that, septic neonates in the treatment group received the adenovirus solution (100 µl, 1×10^{11} PFU) carrying sh-NC or sh-COTL1 intravenously at 1 h after CS injection. Lung tissues and blood samples were obtained 20 h after CS administration. All these procedures were performed as de-scribed previously [24]. The study was approved by Hubei Center for Disease Control and Prevention Laboratory Animal Management and Use Committee (No. 202310149).

Hematoxylin and eosin staining

Formalin (10%) was employed to fix tissues for 10 min, and then the tissues were embedded in paraffin. Next, tissues were cut into 5 µm-thickness sections, and then hematoxylin and eosin (H&E, Beyotime, Shanghai, China) was used to stain the sections. Light microscopy (Olympus, Tokyo, Japan) was applied for evaluation of the slides in order to evaluate lung injury degree. The scoring system was applied by a clinician with bind evaluation [25]. The lung injury score was calculated as the sum of the individual score grades from 0 (minimum) to 1 (mild), 2 (moderate), 3 (severe), and 4 (maximum) for the following three items: thickness of the alveolar walls, infiltration, and aggregation of inflammatory cells, ranging from 0 to 12.

Cell culture and identification

Pulmonary microvascular endothelial cells were isolated from mice according to the recent literature [26]. Then, cells were resuspended and transferred to a flask (T-75). Complete growth medium (7 ml) was added, and then cells were incubated in conditions of 37°C and 5% CO_2. The media were replaced every 2-3 days. The complete growth medium was basal medium supplemented with 100 µg/ml heparin, 100 µg/ml endothelial cell growth supplement, 1× non-essential amino acids and 1 mM sodium pyruvate (Sigma). The basal medium was Dulbecco's Modified Eagle Medium with 4,500 mg/l glucose and 4 mM L-glutamine (DMEM, Invitrogen, USA) supplemented with 20% (v/v) heat-inactivated fetal bovine serum (FBS, Gibco, USA), 100 U/100 µg/ml penicillin/streptomycin (Sigma), and 25 mM HEPES (Sigma). The isolated cells were identified by microscopy and flow cytometry.

Phenotypic characterization of primary pulmonary microvascular endothelial cells

Primary pulmonary microvascular endothelial cells were phenotypically characterized by flow cytometry on a FACSCalibur instrument (BD, Shanghai, China) using the following fluorescein (FITC) and phycoerythrin (PE) conjugated antibodies: CD102 (BD Bioscience, clone MEC 13.3) and CD31 (BD Bioscience, clone 3C4). Appropriately labeled isotype-matched immunoglobulins were used as negative controls. Briefly, 1×10^5 viable cells were incubated with the indicated antibodies for 30 min at 4°C in the dark. Following a washing step in PBS/FCS (10%) cells were analyzed on a FACSCalibur instrument. Dead cells were excluded from the analysis by a propidium iodide co-staining and gating strategy. To mimic NS *in vitro*, cells were treated with lipopolysaccharides (LPS; 100 ng/ml, Sigma) for 24 h [27].

Cell transfection

Pulmonary microvascular endothelial cells were transfected with adenovirus carrying sh-NC (GenePharma, Shanghai, China) or sh-COTL1 (GenePharma), plasmids containing sh-BATF (GenePharma), pcDNA3.1 (oe-NC) or pcDNA3.1-COTL1 (oe-COTL1) using Lipofectamine 2000 (Invitrogen, Shanghai, China) for 24 h. The transfection of cells was observed using an inverted fluorescence microscope (Nikon, Tokyo, Japan) and photographed for recording. In detail, transfection efficiency was evaluated 24 h later. COTL1 shRNA, as well as the negative control, was added to the transfected cells 72 h after GFP expression. Each well received 10 μl of COTL1 shRNA or negative control diluted in 100 μl of sterile water. The GFP level was monitored over the next 24 h.

MTT assay

Cells (3×10^5 cells each well) were seeded overnight. After that, cells were treated with MTT reagent (20 μg/ml, 10 μl; Beyotime) for 2 h, and then 200 μl of supernatants were replaced with the same volume of DMSO. Cell absorbance (490 nm) was analyzed using a microplate reader (Nikon, Tokyo, Japan). The principle for MTT assay was as follows: Succinate dehydrogenase in the mitochondria of living cells can reduce exogenous MTT to water-insoluble blue-violet crystalline formazan and deposit it in the cells, while dead cells do not have this function. Dimethyl sulfoxide (DMSO) can dissolve dirty cells, and its light absorption value was measured at 490 nm by enzyme immunoassay, which can indirectly reflect the number of living cells.

ROS detection

For the purpose of examining the reactive oxygen species (ROS) levels, cells were centrifuged for 10 min (1000 g). Then, cell supernatants were incubated with DCFH-DA (10 μM, BD) for 30 min after being collected. Results were imaged with a fluorescent microscope (Nikon, Tokyo, Japan).

Cell apoptosis detection

Cells were resuspended after centrifugation. Next, PI (5 μl) and FITC (5 μl) were applied to stain cells for 15 min. Flow cytometry (FACScan, ZS-AE7S; BD, Shanghai, China) was employed for analysis of apoptosis.

ELISA

Interleukin 1β and IL-6 levels were assessed using an enzyme-linked immunosorbent assay (ELISA) kit (Abcam, Shanghai, China). In detail, primary antibodies were employed for pre-coating plates overnight. FBS (10%) was used in blocking the plates for 1 h after removing supernatants. Next, samples were added to the plates for 2 h.

Subsequently, we replaced supernatants with secondary antibodies (Goat Anti-Rabbit IgG, cat.no ab6728, Abcam, 1 : 1000). After incubation, supernatants were removed, and plates were exposed to HCL (10 nM). Finally, cell absorbance was determined at 490 nm using a microreader (Invitrogen). The information of primary antibodies was as follows: anti-IL-1β (cat. no ab241673, Abcam, 1 : 200), anti-IL-6 (cat. no ab222503, Abcam, 1 : 200).

Biochemical analysis

Malondialdehyde (MDA) and superoxide dismutase (SOD) levels in cells or lung tissues of mice were assessed using biochemical kits (MultiSciences Lianke Biotech Co., Ltd) in accordance with the protocol of the manufacturer.

Chromatin immunoprecipitation assay

The binding of COTL1 with BATF was assessed using the EZ-ChIP Kit. Formaldehyde was applied in incubating cells to obtain DNA-protein crosslinks. After DNA fragmentation, BATF (1 : 50, cat. no #3244, Santa Cruz, MA, USA) or IgG (1 : 50, cat. no ab172730, Abcam) antibody was applied in immunoprecipitating samples. Finally, western blot was applied to investigate precipitated chromatin.

Dual luciferase report assay

The prediction of JASPAR (https://jaspar.elixir.no/) indicated that BATF had binding sites with the COTL1 promoter. The sequences of COTL1 containing the sites of BATF were amplified and cloned into the pGBKT7. PRL-3 Dual-Luciferase Vectors (Promega Corporation, Shanghai, China) to construct COTL1-WT vectors. The mutant (MUT) COTL1 sequence involving binding sites of BATF were generated with the Mutagenesis kit (Q5 Site-Directed) to construct COTL1-MUT. COTL1-WT or COTL1-MUT vector was added into cells with sh-BATF or sh-NC with Lipofectamine 2000 (Invitrogen). After incubation for 48 h, Lipofectamine 2000 (Invitrogen) was employed for detection of luciferase activity. Renilla luciferase activity was used for normalizing data.

RT-qPCR

Total RNA was isolated from cells or tissues using TRIzol Reagent (Takara, Tokyo, Japan). PrimeScript RT (cat. no. R312; Vazyme Biotech Co., Ltd.) was employed in synthesizing cDNA. SYBR Green (Beyotime) was used in RT-qPCR detection with the ABI7500 system (Applied Biosystems Inc., USA). RT-qPCR was applied as follows: 94°C for 2 min, followed by 35 cycles (94°C for 30 s and 55°C for 45 s). The $2^{-\Delta\Delta CT}$ method was applied for data quantification. Primers originated from GenePharma. COTL1: F: 5'-AACTGTGACAACACACCCGT-3' and R: 5'-CCTGTCTTGGCCACAGATGAT-3'. β-actin:

F: 5'-CATCCGTAAAGACCTCTATGCCAAC-3' and R: 5'-ATGGTGCCACCGATCCACA-3'.

Western blot

RIPA (Beyotime) was employed in isolating protein. A BCA kit (Invitrogen) was applied for calculating protein concentration. Subsequently, SDS-PAGE (10%) was employed for separating the proteins, and then separated proteins were transferred onto PVDF membranes (Beyotime). Primary antibodies were applied for incubation of the membranes overnight after blocking for 1 h. Secondary anti-rabbit antibody (Abcam; 1 : 5000) was employed for incubation of the membranes for 1 h. The Odyssey Imaging System was used in scanning the membranes and Odyssey v2.0 was used in analyzing the data. Primary antibodies were as follows: anti-COTL1 (cat. no. ab235833, 1 : 1000), anti-cleaved caspase 3 (cat. no. ab214430, 1 : 5000), anti-pro-caspase (cat. no. ab32499, 1 : 10000) anti-Bcl-2 (cat. no. ab182858, 1 : 2000), anti-Bax (cat. no. ab32503, 1 : 1000), anti-p38 (cat. no. ab31828, 1 : 1000), anti-p-p38 (cat. no. ab195049, 1 : 1000), anti-p65 (cat. no. ab32536, 1 : 1000), anti-p-p65 (cat. no. ab76302, 1 : 1000) and anti-GAPDH (cat. no. ab8245, 1 : 1000). All antibodies originated from Abcam (Shanghai, China).

Statistical analysis

Three independent experiments were applied in each group and mean ± standard deviation (SD) was employed for expressing the data. Student's t-test (only 2 groups) or one-way analysis of variance (ANOVA) followed by Tukey's test (more than 2 groups) was applied to analyze the differences. SPSS 20.0 (NIH, USA) was used for data analysis. $P < 0.05$ was considered to indicate a significant difference.

Results

COTL1 silencing alleviated lung injury in septic neonates

It was reported that the level of COTL1 was upregulated in patients with sepsis [12]. Thus, to detect the function of COTL1 in NS, an animal study was employed. As shown in Supplementary Figure 2, the lung tissues in sham mice appeared pink with no congestion or edema; however, CS treatment significantly enhanced the volume of lung tissues, transformed pink to dark red and increased the congestion and edema. CS treatment significantly induced thickening of lung septa with inflammatory infiltration and increase of lung injury scores, while silencing of COTL1 significantly rescued this phenomenon (Fig. 1A, B). Additionally, COTL1 level in lung tissues of septic neonates was significantly upregulated after CS treatment, but it was partially abolished by COTL1 shRNA (Fig. 1C, D).

Consistently, CS upregulated interleukin (IL)-1β and IL-6 levels in mice, which was markedly inhibited after silencing of COTL1 (Fig. 1E). In contrast, CS administration significantly induced the downregulation of SOD activity and upregulation of MDA level, while the impact of CS treatment was overturned by sh-COTL1 (Fig. 1F). Furthermore, CS administration greatly increased the ratio of cleaved caspase-3/pro-caspase 3 and the level of Bax and decreased the expression of Bcl-2 in tissues of septic neonates (Fig. 1G). Nevertheless, the effect of CS treatment on these three proteins was attenuated by downregulation of COTL1 (Fig. 1G). Collectively, knockdown of COTL1 attenuated lung injury in septic neonates.

Silencing of COTL1 markedly alleviated LPS-induced inflammatory responses

Primary pulmonary microvascular endothelial cells were identified using microscopy and flow cytometry. As shown in Figure 2A, the isolated cells exhibited a cobblestone shape, and it was consistent with the feature of endothelial cells. In addition, the proportion of cells that stained positively for CD31 and CD102 (two markers of endothelial cells) was nearly 91.08% (Fig. 2B). Next, the fluorescence microscope was used to detect the transfection efficiency. As expected, about 85% of cells transfected with sh-COTL1 and sh-NC exerted notable expression of GFP (Fig. 2C). Thus, it could be suggested sh-NC and sh-COTL1 were successfully transfected into cells. To further confirm the function of COTL1 in NS, cells were exposed to LPS. It was observed that the viability of cells was significantly reduced by LPS treatment, which was reversed by knockdown of COTL1 (Fig. 2D). COTL1 level was significantly upregulated by LPS treatment, and sh-COTL1 reversed this phenomenon (Fig. 2E, F). Moreover, IL-1β and IL-6 levels in supernatants were markedly elevated by LPS treatment, which were abolished after COTL1 knockdown (Fig. 2G). Thus, knockdown of COTL1 alleviated LPS-induced inflammatory responses during the progression of NS.

Downregulation of COTL1 alleviated LPS-induced oxidative stress and apoptosis in pulmonary microvascular endothelial cells

Next, the effect of COTL1 on oxidative stress and apoptosis of pulmonary microvascular endothelial cells was further explored. As illustrated in Figure 3A, LPS stimulation significantly increased the ROS level in cells, which was abolished by downregulation of COTL1. LPS significantly inhibited SOD activity and increased MDA level in cells, and sh-COTL1 partly inhibited the effect of LPS treatment (Fig. 3B). Moreover, LPS treatment greatly promoted cell apoptosis, which was inhibited by silencing of COTL1 (Fig. 3C). Finally, LPS treatment greatly elevated the level of Bax and the ratio of cleaved caspase-3/pro-caspase 3 and decreased the expression
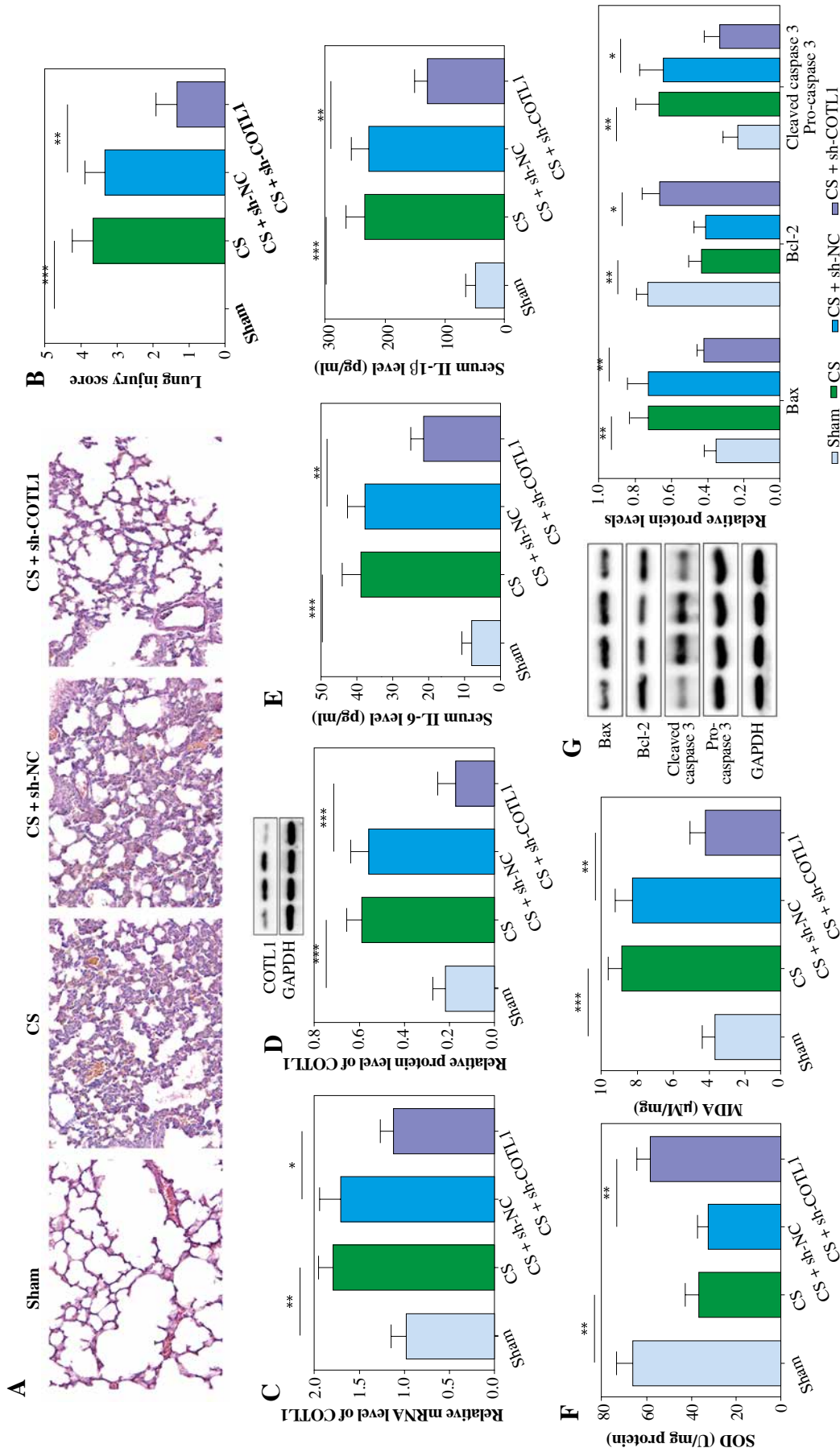
Fig. 1. Knockdown of COTL1 significantly alleviated the lung injury in septic neonates. Septic neonates in the treatment group received the adenovirus solution (100 µl, 1 × 10^{11} PFU) carrying sh-NC or sh-COTL1 intravenously at 1 h after CS injection. **A)** The histological changes in lung tissues of septic neonates were observed using H&E staining. **B)** The lung injury scores were evaluated. **C)** The mRNA level of COTL1 in septic neonates was tested by RT-qPCR. **D)** The protein level of COTL1 in septic neonates was investigated by western blot. **E)** The levels of IL-1β and IL-6 in serum of septic neonates were assessed using ELISA. **F)** The levels of SOD and MDA were evaluated by commercial kits. **G)** The protein levels of Bax, cleaved caspase 3, pro-caspase 3 and Bcl-2 in tissues of septic neonates were determined by western blot. $N = 6$. *$p < 0.05$, **$p < 0.01$, ***$p < 0.001$
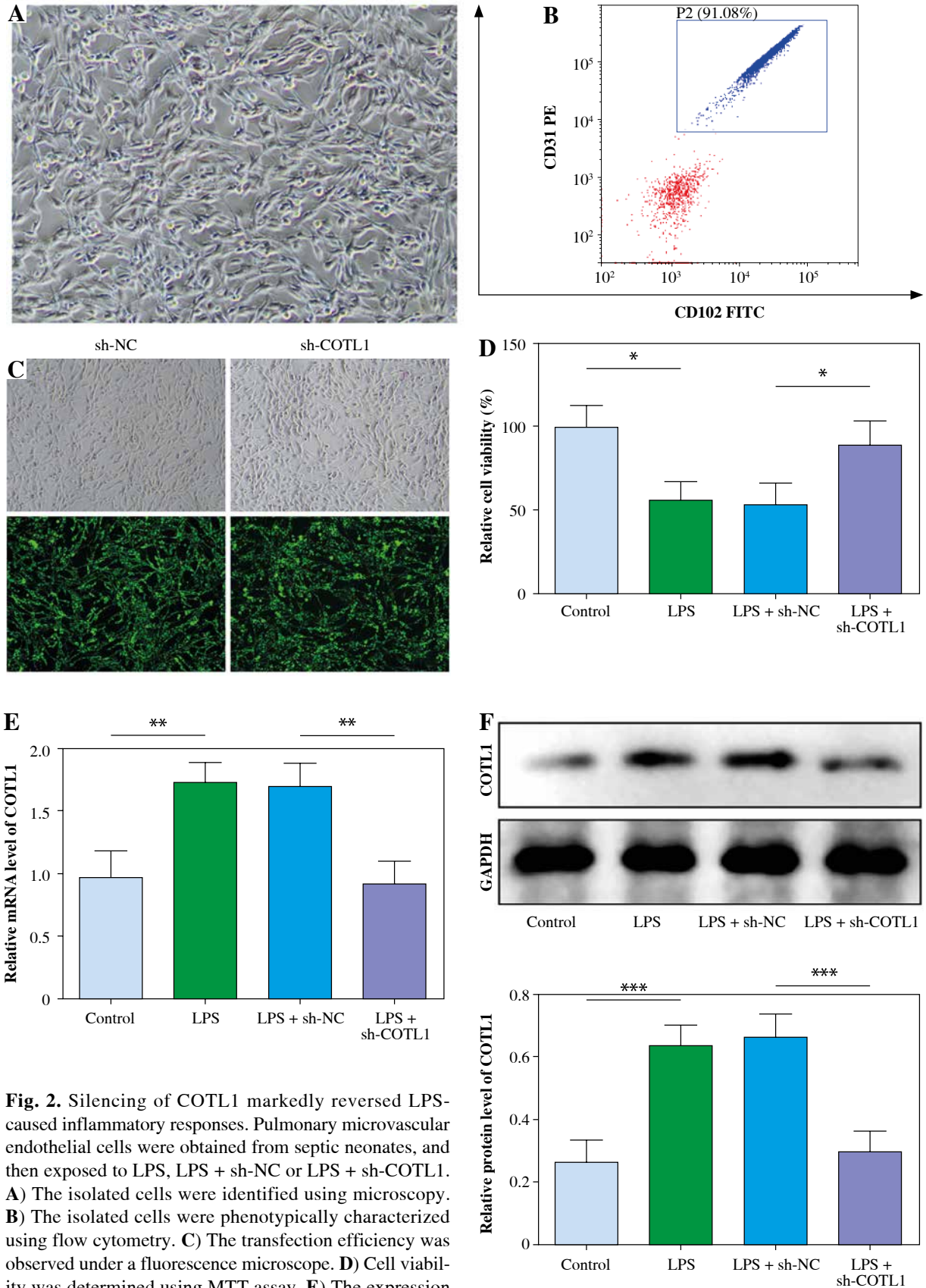
Fig. 2. Silencing of COTL1 markedly reversed LPS-caused inflammatory responses. Pulmonary microvascular endothelial cells were obtained from septic neonates, and then exposed to LPS, LPS + sh-NC or LPS + sh-COTL1. **A**) The isolated cells were identified using microscopy. **B**) The isolated cells were phenotypically characterized using flow cytometry. **C**) The transfection efficiency was observed under a fluorescence microscope. **D**) Cell viability was determined using MTT assay. **E**) The expression of COTL1 was tested using RT-qPCR. **F**) The protein level of COTL1 in cells was determined using western blot.
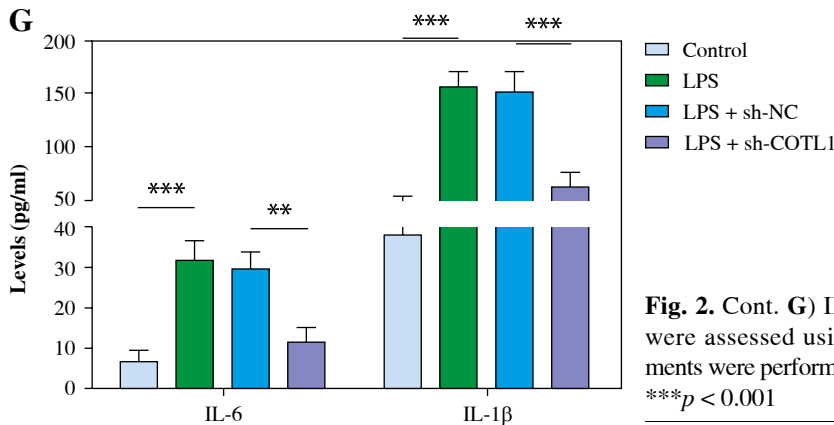
G

of Bcl-2 in cells, and sh-COTL1 markedly reversed this phenomenon (Fig. 3D). Taken together, downregulation of COTL1 alleviated LPS-caused oxidative stress and apoptosis in pulmonary microvascular endothelial cells.

BATF could activate MAPK/NF-κB signaling through transcriptionally upregulating COTL1

Subsequently, we further investigate the upstream underlying function of COTL1 in NS. The data showed that BATF had binding sites with the COTL1 promoter (Fig. 4A). Next, ChIP and dual luciferase assays were applied to confirm the relation between BATF and COTL1. In Figure 4B, the enrichment of COTL1 was markedly elevated by BATF. Additionally, luciferase activity in COTL1-WT was significantly downregulated by sh-BATF, while BATF silencing had a limited influence on luciferase activity in COTL1-MUT (Fig. 4C). The levels of COTL1, p-p38 and p-p65 in cells were markedly upregulated after LPS stimulation, an effect reversed by sh-BATF (Fig. 4D, E). The impact of sh-BATF was abolished by COTL1 overexpression (Fig. 4D, E). In summary, BATF could transcriptionally upregulate COTL1 *via* activation of MAPK/NF-κB signaling.

BATF knockdown inhibited LPS-caused inflammatory responses, oxidative stress and apoptosis

To further confirm whether BATF could play a role in NS *via* regulation of COTL1, cells were treated with sh-BATF, and then exposed to oe-COTL1. As indicated in Figure 5A, LPS treatment-inhibited cell viability was significantly reversed by sh-BATF, while the impact was abolished by oe-COTL1. Consistently, the pro-inflammatory effect of LPS treatment was significantly reduced by silencing of BATF, while oe-COTL1 partly weakened the anti-inflammatory effect of BATF shRNA (Fig. 5B). The effect of LPS on ROS, SOD and MDA was suppressed by sh-BATF, which was abolished by oe-COTL1

(Fig. 5C, D). Furthermore, knockdown of BATF could inhibit the apoptotic effect of LPS on pulmonary microvascular endothelial cells by regulating Bax, Bcl-2 and the ratio of cleaved caspase-3/pro-caspase 3, while COTL1 upregulation abolished this impact of BATF knockdown (Fig. 5E, F). To sum up, BATF knockdown inhibited LPS-caused inflammatory responses, oxidative stress and apoptosis.

Discussion

Progression of NS seriously threatens the health of infants, and the survival rate of NS patients still remains low [28]. In addition, lung injury is a major cause of sepsis that seriously threatens the health of patients with sepsis [29]. Thus, it is necessary to explore new therapeutic strategies for alleviating lung injury in NS. This study found that knockdown of BATF could transcriptionally regulate COTL1 to exert its pro-septic function through MAPK/NF-κB signaling. Hence, our study is the first to illustrate the function of COTL1 in NS, which provided a new insight into exploring a therapeutic target against NS.

It was demonstrated that COTL1 could bind to 5-lipoxygenase and F-actin, which is involved in inflammation and cancer [30, 31]. In addition, this research revealed that COTL1 inhibited LPS-induced oxidative stress and inflammation. COTL1 is involved in sepsis progression and lung injury. For example, COTL1 level was positively associated with the severity of NS [32], but the function of COTL1 in NS is not clear. Consistently, our finding demonstrated that COTL1 silencing attenuated lung injury in septic neonates. In a previous study, CS was used to establish the model of NS [33]. Thus, CS was selected for constructing an *in vivo* model of NS in our research. Moreover, silencing of COTL1 alleviated LPS-induced inflammatory responses in pulmonary microvascular endothelial cells of septic neonates. Collectively, COTL1 is closely correlated with the progression of NS. Moreover, MAPK/NF-κB activation could lead to progression of NS, and its upregulation could also induce inflammation and oxida-
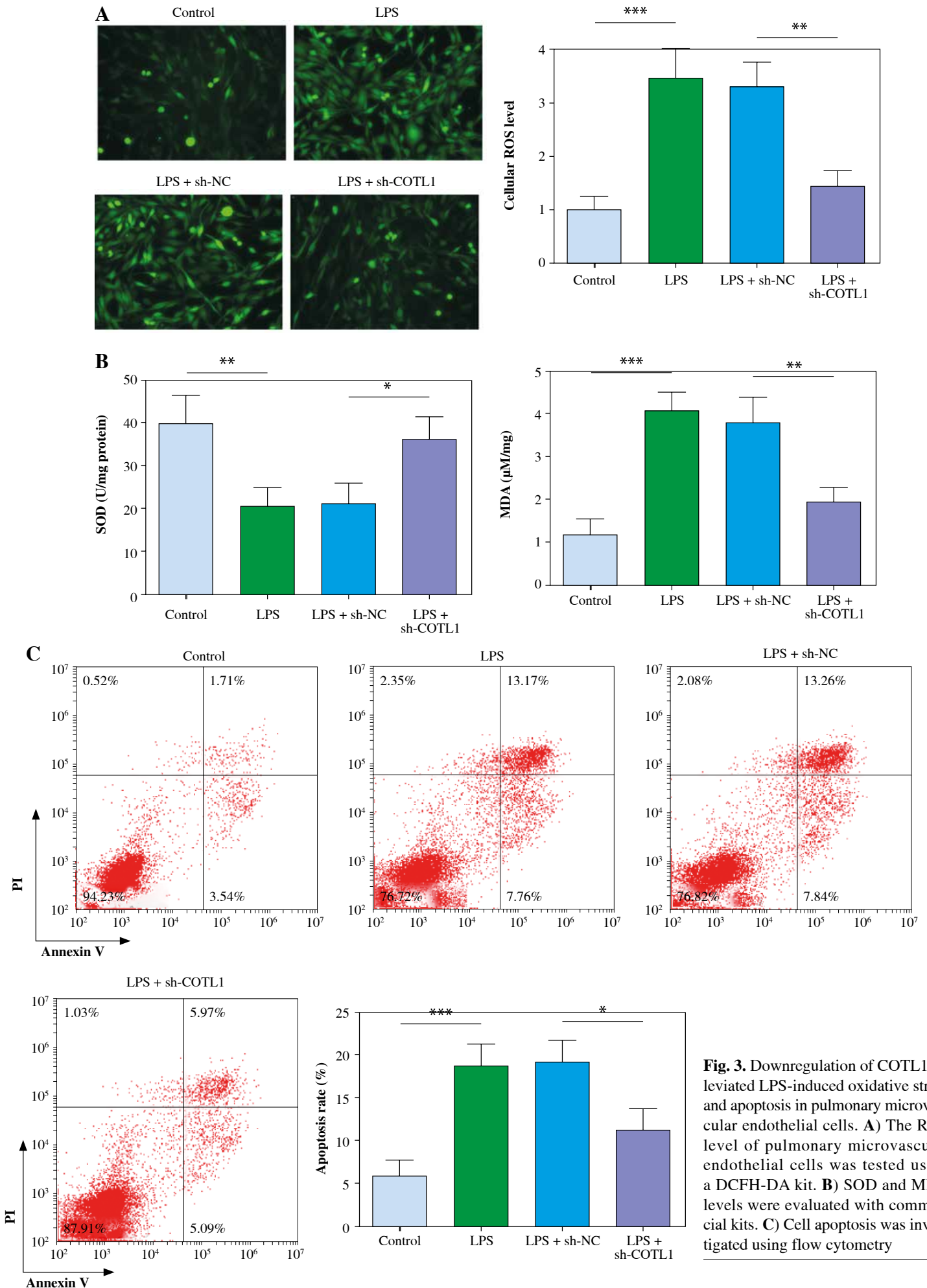
Fig. 3. Downregulation of COTL1 alleviated LPS-induced oxidative stress and apoptosis in pulmonary microvascular endothelial cells. **A)** The ROS level of pulmonary microvascular endothelial cells was tested using a DCFH-DA kit. **B)** SOD and MDA levels were evaluated with commercial kits. **C)** Cell apoptosis was investigated using flow cytometry
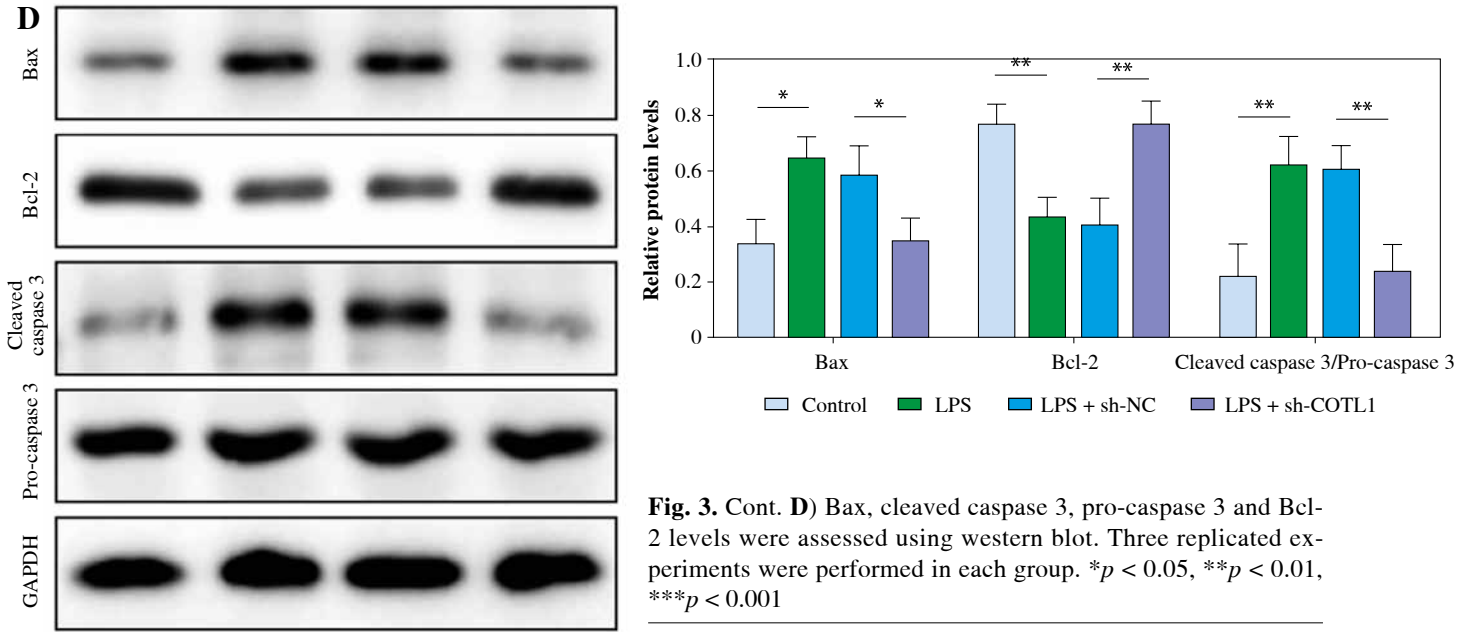
Fig. 3. Cont. **D**) Bax, cleaved caspase 3, pro-caspase 3 and Bcl-2 levels were assessed using western blot. Three replicated experiments were performed in each group. *$p < 0.05$, **$p < 0.01$, ***$p < 0.001$
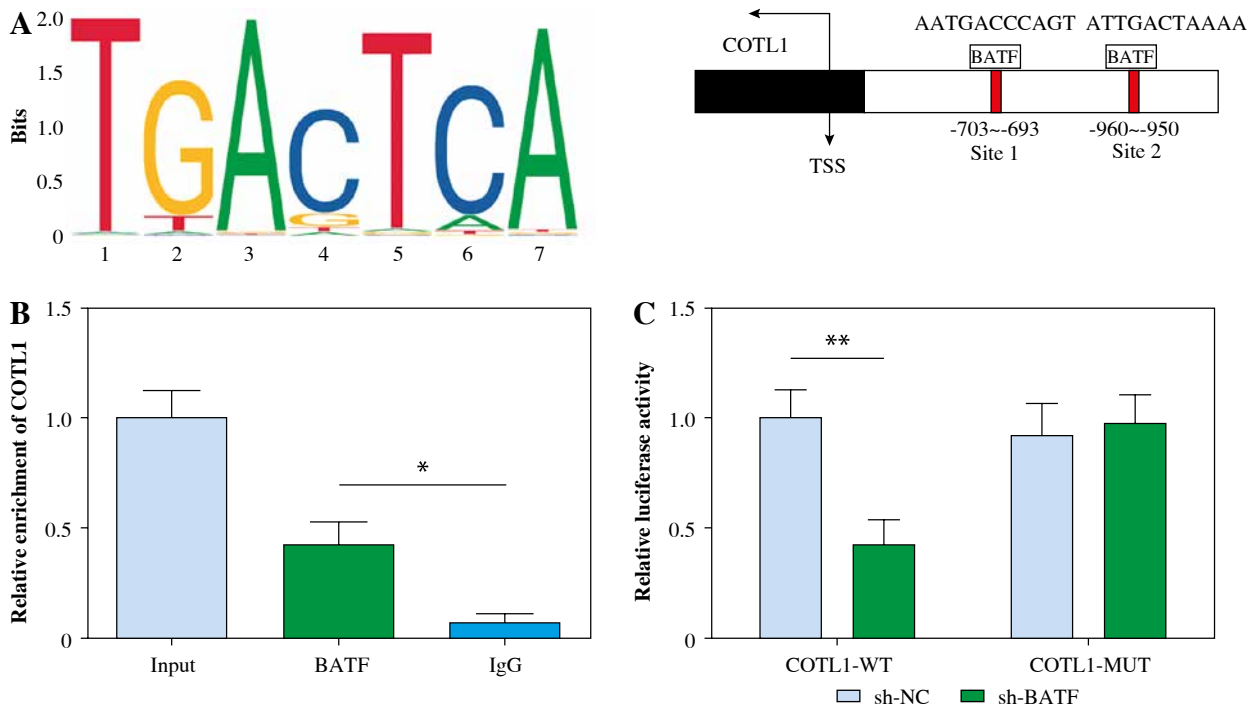

Fig. 4. BATF could activate MAPK/NF-κB signaling through transcriptionally upregulating COTL1. **A**) The binding sites between BATF and COTL1 were predicted using JASPAR. **B**) The enrichment of COTL1 was tested using ChIP assay. **C**) The luciferase activity in COTL1-WT/MUT was assessed using dual luciferase report assay. Pulmonary microvascular endothelial cells were treated with LPS, LPS + sh-NC, LPS + sh-BATF, LPS + sh-BATF + oe-NC or LPS + sh-BATF + oe-COTL1
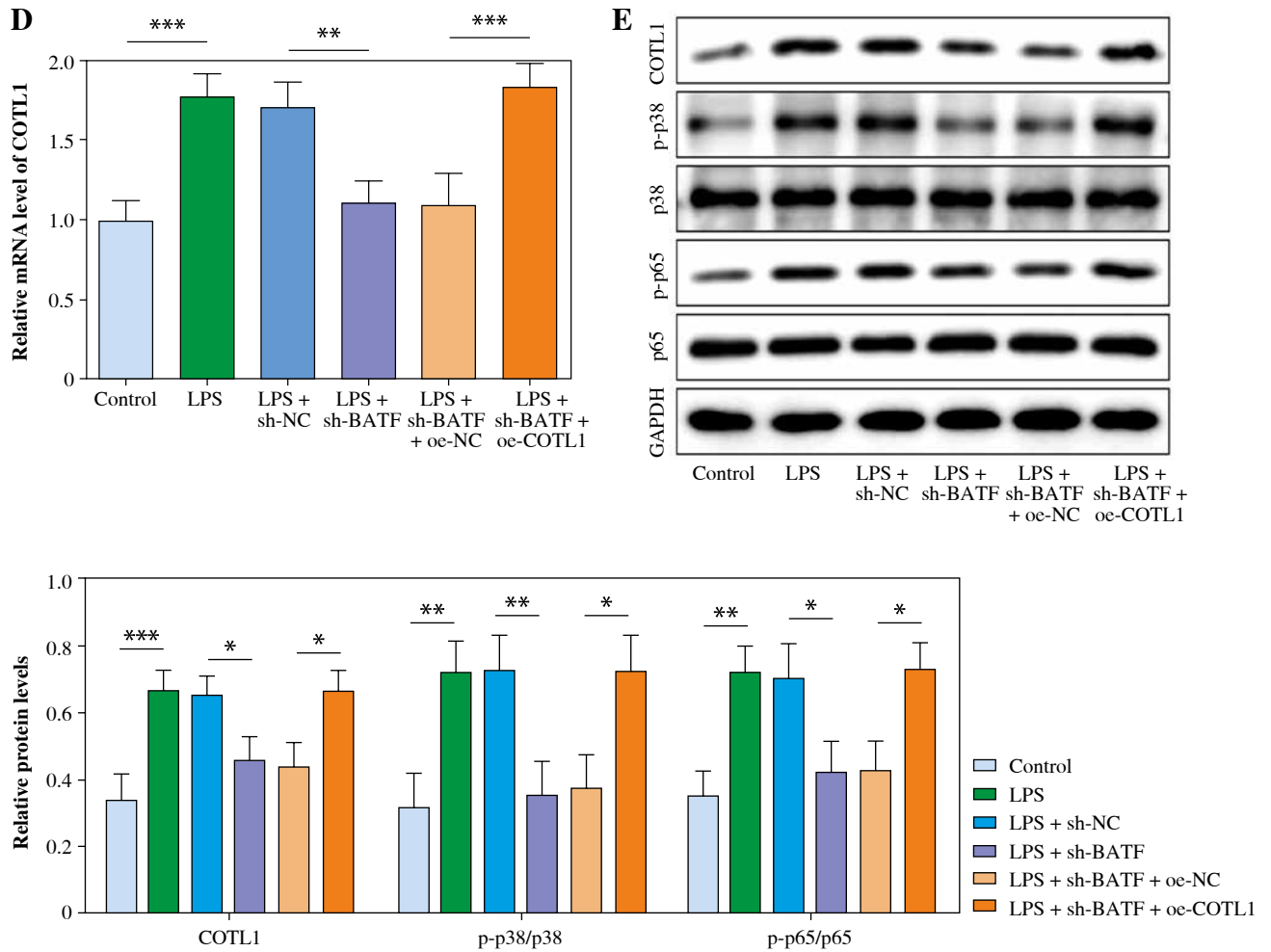
Fig. 4. Cont. **D**) COTL1 level in cells was determined using RT-qPCR. **E**) COTL1, p38, p-p38, p65 and p-p65 levels in cells were investigated using western blot. Three replicated experiments were performed in each group. *$p < 0.05$, **$p < 0.01$, ***$p < 0.001$

tive stress [34, 35]. Remarkably, our research revealed that overexpression of COTL1 could aggravate the progression of NS through activating MAPK/NF-κB signaling.

BATF is a transcriptional factor which participates in inflammation and lung injury [23, 36], and it is confirmed to be a key mediator in sepsis [22]. In addition, it was revealed that BATF could regulate the progression of multiple diseases through transcriptional regulation with its downstream mRNAs. For instance, Zhang *et al.* found that BATF could relieve the development of hepatic steatosis through inhibiting PD1 [21]; BATF could stabilize Th17 cell development through transcriptionally upregulating STAT5 [37]. Consistently, this research found that BATF could transcriptionally upregulate COTL1 expression. Moreover, sh-BATF could inhibit oxidative stress, apoptosis and inflammatory responses. Our study is the first to illustrate the relationship between BATF5 and COTL1

in NS. Indeed, the present study will be strengthened in clinical practice if conditions permit in future. Meanwhile, it is worth exploring whether MAPK/NF-κB signaling can affect COTL1-mediated NS progression. Hence, more investigations are essential in future.

In summary, BATF silencing alleviates lung injury in septic neonates through transcriptional upregulation of COTL1. Thus, this study might provide a new theoretical basis for discovering new therapeutic methods in clinical practice.

Funding
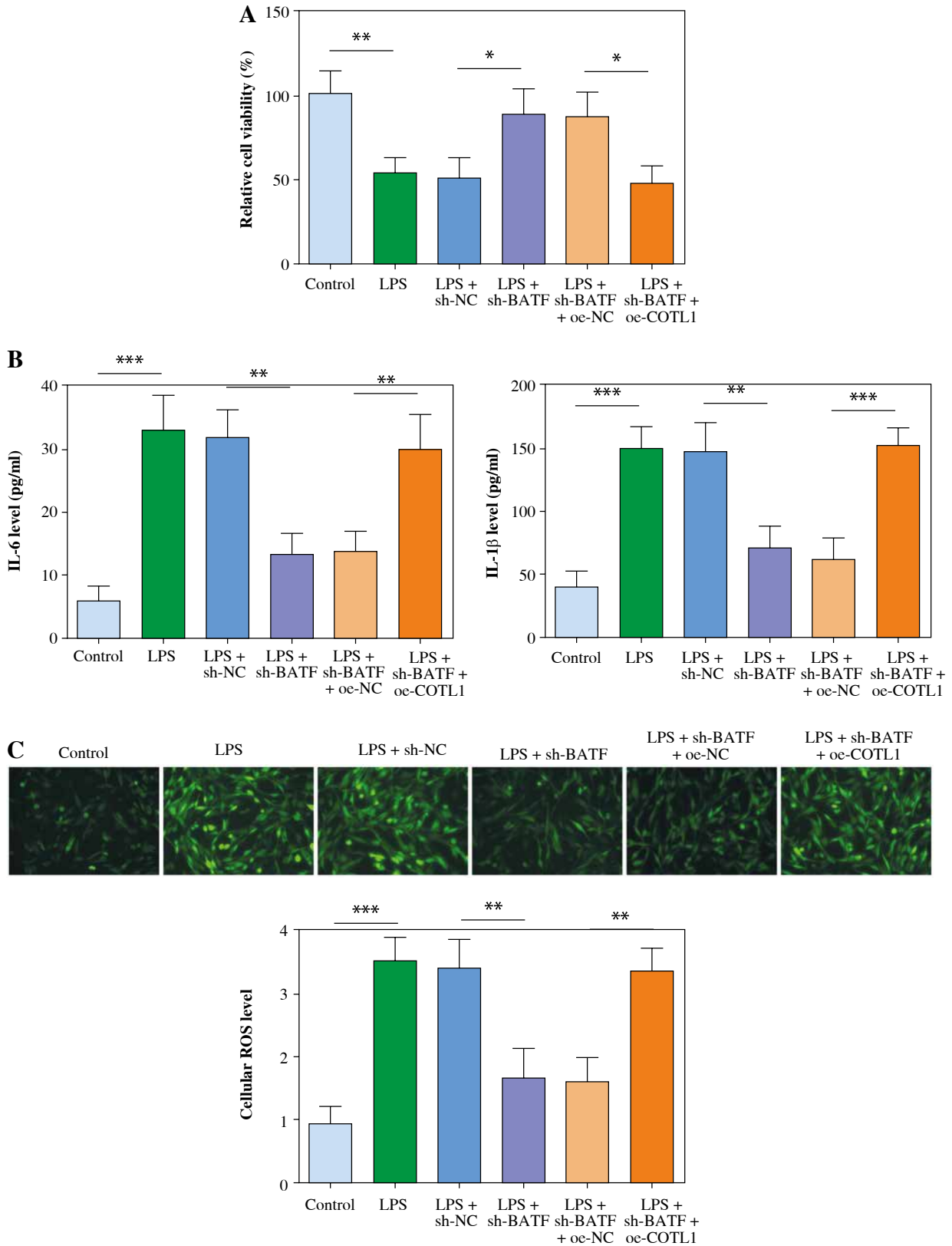
Jihui Zhang, Huimin Jiang

Fig. 5. BATF knockdown could inhibit LPS-caused inflammatory responses, oxidative stress and apoptosis. Pulmonary microvascular endothelial cells were obtained from septic neonates, and then treated with LPS, LPS + sh-NC, LPS + sh-BATF, LPS + sh-BATF + sh-NC or LPS + sh-BATF + sh-COTL1. **A)** Cell viability was assessed using MTT assay. **B)** IL-1β and IL-6 levels in cell supernatants were evaluated using ELISA. **C)** ROS level of pulmonary microvascular endothelial cells was tested using a DCFH-DA kit
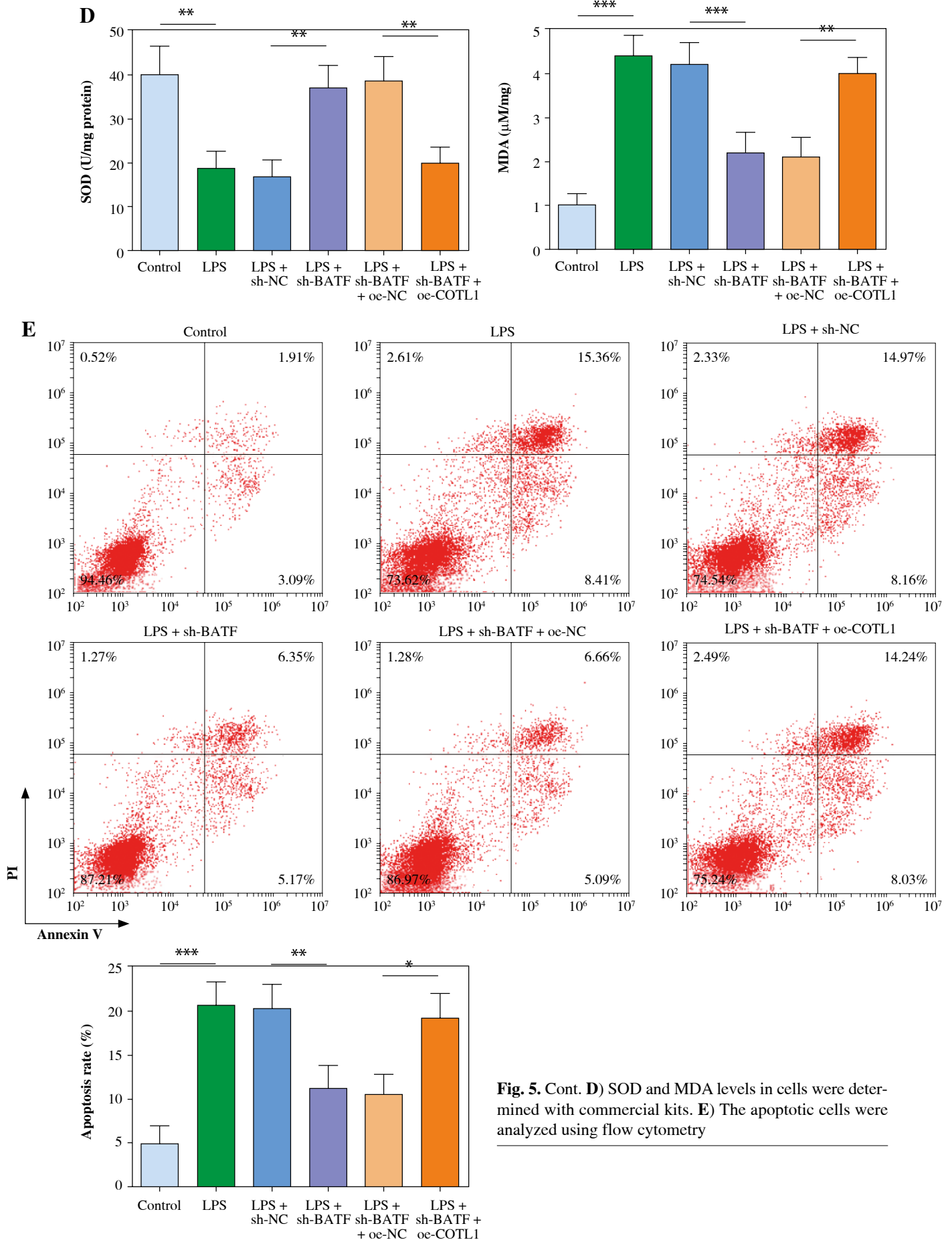
Fig. 5. Cont. **D**) SOD and MDA levels in cells were determined with commercial kits. **E**) The apoptotic cells were analyzed using flow cytometry
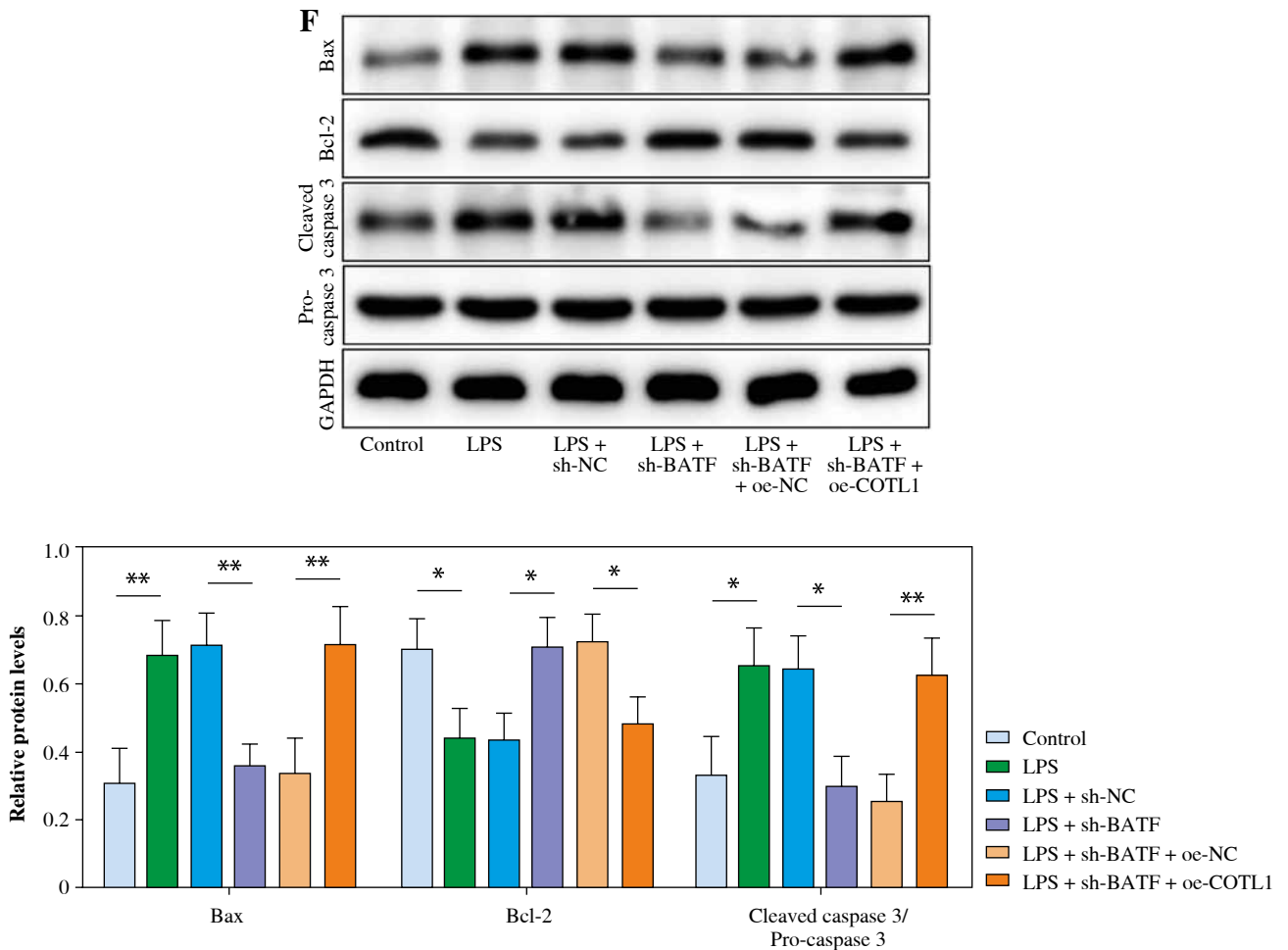
Fig. 5. Cont. **F**) The protein expression levels of Bax, cleaved caspase 3, pro-caspase 3 and Bcl-2 in cells were tested using western blot. Three replicated experiments were performed in each group. *$p < 0.05$, **$p < 0.01$, ***$p < 0.001$

Disclosures

The study was approved by Hubei Center for Disease Control and Prevention Laboratory Animal Management and Use Committee (No. 202310149).

The authors declare no conflict of interest.

References

1. Dong Y, Basmaci R, Titomanlio L, et al. (2020): Neonatal sepsis: within and beyond China. Chin Med J (Engl) 133: 2219-2228.
2. Bethou A, Bhat BV (2022): Neonatal sepsis-newer insights. Indian J Pediatr 89: 267-273.
3. Cantey JB, Lee JH (2021): Biomarkers for the diagnosis of neonatal sepsis. Clin Perinatol 48: 215-227.
4. Zhang H, Liu J, Zhou Y, et al. (2022): Neutrophil extracellular traps mediate mA modification and regulates sepsis-associated acute lung injury by activating ferroptosis in alveolar epithelial cells. Int J Bio Sci 18: 3337-3357.
5. Zhang J, Zheng Y, Wang Y, et al. (2022): YAP1 alleviates sepsis-induced acute lung injury inhibiting ferritinophagy-mediated ferroptosis. Front Immunol 13: 884362.
6. Abu-Sultaneh S, Iyer N, Fernández A, et al. (2023): Executive summary: International clinical practice guidelines for pediatric ventilator liberation, a pediatric acute lung injury and sepsis investigators (PALISI) network document. Am J Respir Crit Care Med 207: 17-28.
7. Wang X, Bai Y, Wang B (2024): Coactosin-like protein 1 (COTL1) could be an immunological and prognostic biomarker: From pan-cancer analysis to low-grade glioma validation. J Inflamm Res 2024; 17: 1805-1820.
8. Xia L, Xiao X, Liu W, et al. (2018): Coactosin-like protein CLP/Cotl1 suppresses breast cancer growth through activation of IL-24/PERP and inhibition of non-canonical TGFβ signaling. Oncogene 37: 323-331.
9. Tan D, Chen XX, Bai T, et al. (2020): Sevoflurane up-regulates microRNA-204 to ameliorate myocardial ischemia/reperfusion injury in mice by suppressing Cotl1. Life Sci 259: 118162.

10. Biwei M, Lirong Z, Qi W, et al. (2024): Diagnostic accuracy of pancreatic stone protein in patients with sepsis: a systematic review and meta-analysis. BMC Infect Dis 24: 472.

11. Weihua S, Xiaoli L, Yongxing S, et al. (2023): PILRA is associated with immune cells infiltration in atrial fibrillation based on bioinformatics and experiment validation. Front Cardiovasc Med 10:1082015.

12. Rashi S, Navkiran K, Rakhi M, et al. (2022): Plasma proteomic analysis identified proteins associated with faulty neutrophils functionality in decompensated cirrhosis patients with sepsis. Cells 11: 1745.

13. Lan T, Chen B, Hu X, et al. (2024): Tianhuang formula ameliorates liver fibrosis by inhibiting CCL2-CCR2 axis and MAPK/NF-κB signaling pathway. J Ethnopharmacol 321: 117516.

14. Wen J, Peng H, Wang D, et al. (2023): Lipopolysaccharides protect mesenchymal stem cell against cardiac ischemia-reperfusion injury by HMGB1/STAT3 signaling. J Geriatr Cardiol 20: 801-812.

15. Guo Y, Zhang H, Lv Z, et al. (2023): Up-regulated CD38 by daphnetin alleviates lipopolysaccharide-induced lung injury via inhibiting MAPK/NF-κB/NLRP3 pathway. Cell Commun Signal 21: 66.

16. Wang J, Xue X, Zhao X, et al. (2024): Forsythiaside A alleviates acute lung injury by inhibiting inflammation and epithelial barrier damages in lung and colon through PPAR-γ/RXR-α complex. J Adv Res 60: 183-200.

17. Liu Z, Huang X, Guo H, et al. (2023): Design, synthesis fusidic acid derivatives alleviate acute lung injury via inhibiting MAPK/NF-κB/NLRP3 pathway. Eur J Med Chem 259: 115697.

18. Popp A, Hettich J, Gebhardt JCM (2021): Altering transcription factor binding reveals comprehensive transcriptional kinetics of a basic gene. Nucleic Acids Res 49: 6249-6266.

19. Miravet-Verde S, Lloréns-Rico V, Serrano L (2017): Alternative transcriptional regulation in genome-reduced bacteria. Curr Opin Microbiol 39: 89-95.

20. Titcombe P, Silva Morales M, Zhang N, et al. (2023): BATF represses BIM to sustain tolerant T cells in the periphery. J Exp Med 220: e202320183.

21. Zhang Z, Liao Q, Pan T, et al. (2023): BATF relieves hepatic steatosis by inhibiting PD1 and promoting energy metabolism. Elife 12: RP88521.

22. Guo H, Ni M, Xu J, et al. (2021): Transcriptional enhancement of GBP-5 by BATF aggravates sepsis-associated liver injury via NLRP3 inflammasome activation. FASEB J 35: e21672.

23. Watanabe T, Lam C, Oliver J, et al. (2023): Donor Batf3 inhibits murine lung allograft rejection and airway fibrosis. Mucosal Immunol 16: 104-120.

24. Bolognese A, Yang W, Hansen L, et al. (2018): Inhibition of necroptosis attenuates lung injury and improves survival in neonatal sepsis. Surgery 27: S0039-6060(18)30096-5.

25. Zhang Y, Zhang J, Ren Y, et al. (2021): Luteolin suppresses sepsis-induced cold-inducible RNA-binding protein production and lung injury in neonatal mice. Shock 55: 268-273.

26. Wong E, Nguyen N, Hellman J (2021): Isolation of primary mouse lung endothelial cells. J Vis Exp 177: 10.3791/63253.

27. Mai J, He Q, Liu Y, et al. (2023): Hyperoside attenuates sepsis-induced acute lung injury (ALI) through autophagy regulation and inflammation suppression. Mediators Inflamm 2023: 1257615.

28. Chen X, He H, Wei H, et al. (2023): Risk factors for death caused by early onset sepsis in neonates: a retrospective cohort study. BMC Infect Dis 23: 844.

29. Mas-Celis F, Olea-López J, Parroquin-Maldonado JA (2021): Sepsis in trauma: A deadly complication. Arch Med Res 52: 808-816.

30. Kwak M, Hwang C, Cha J, et al. (2023): Single-cell network-based drug repositioning for discovery of therapies against anti-tumour necrosis factor-resistant Crohn's disease. Int J Mol Sci 24: 14099.

31. Wang B, Zhao L, Chen D (2022): Coactosin-like protein in breast carcinoma: Friend or foe? J Inflamm Res 15: 4013-4025.

32. Sehgal R, Kaur N, Maiwall R, et al. (2022): Plasma proteomic analysis identified proteins associated with faulty neutrophils functionality in decompensated cirrhosis patients with sepsis. Cells 11: 1745.

33. Denorme F, Rustad J, Portier I, et al. (2023): Neutrophil extracellular trap inhibition improves survival in neonatal mouse infectious peritonitis. Pediatr Res 93: 862-869.

34. Xu G, Chen H, Cong Z, et al. (2024): Promotion of transcription factor EB-dependent autophagic process by curcumin alleviates arsenic-caused lung oxidative stress and inflammation in mice. J Nutr Biochem 125: 109550.

35. Jiang X, Zhu X, Liu Y, et al. (2023): Diallyl trisulfide and its active metabolite allyl methyl sulfone attenuate cisplatin-induced nephrotoxicity by inhibiting the ROS/MAPK/NF-κB pathway. Int Immunopharmacol 127: 111373.

36. Wu X, Kasmani MY, Zheng S, et al. (2022): BATF promotes group 2 innate lymphoid cell-mediated lung tissue protection during acute respiratory virus infection. Sci Immunol 7: eabc9934.

37. Pham D, Silberger D, Nguyen K, et al. (2023): Batf stabilizes Th17 cell development via impaired Stat5 recruitment of Ets1-Runx1 complexes. EMBO J 42: e109803.